Detection and identification of ore grindability in a semiautogenous grinding circuit model using wavelet transform variances of measured variables

G.D. Gonzalez [a,b,*], D. Miranda [a], A. Casali [b], G. Vallebuona [b]

[a] *Electrical Engineering Department, University of Chile, Av. Tupper 2007, Santiago, Chile*
[b] *Mining Engineering Department, University of Chile, Av. Tupper 2069, Santiago, Chile*

Keywords:
Semiautogenous grinding
Dynamic models
Statistical methods
Principal component analysis
Wavelets

A B S T R A C T

A reduced dimension dynamic model subject to random disturbances for a semiautogenous grinding (SAG) circuit is developed that is able to handle changes in the characteristics of the new feed ore. This dynamic model, which is adjusted using data from a large mineral processing plant, has been developed with the objective of being useful for design and testing of fault identification and detection (FDI) systems, soft-sensors, automatic control systems, etc. The reduced dimension is a requirement in order to be able to obtain in a reasonable time statistical results to evaluate such systems. In this paper this SAG circuit dynamic model is used to test a method for detecting changes and identifying the grindability of the ore being processed by the SAG circuit. The method used — based on the variance of the continuous wavelet transform of measured circuit variables — incorporates improvements of a previous method. Results show that a step change of new feed ore is detected in about 30 to 80 min depending on the grindability change. This result may be considered to be adequate when taking into account that the response time for the mill hold-up to attain a new equilibrium value after the ensuing transient is of about 3 h. Identification of grindability in stationary operation gives near 100% of correct classification under the analysed conditions. The sensitivity of the FDI method to changes in circuit characteristics is also assessed and acceptable results are obtained.

1. Introduction

The principal aim of this work is to develop a method for on-line detection and identification of grindability of the ore being processed by a SAG mill. To test this procedure a SAG circuit model is developed which is able to handle changes in the characteristics of the fresh feed ore. The purpose of the model of the SAG mill circuit developed here is that it should behave like a real circuit from a qualitative point of view, and that from a quantitative point of view it should be within what might be expected of such circuits. Therefore the model must reproduce the main features of actual SAG mills in general, so that it may be used for designing and testing identification and detection systems for faults and operating conditions, automatic control systems, test soft-sensor designs, etc. The model developed here is of reduced dimension (i.e., five) in order to be able to obtain in reasonable time statistical results to evaluate such systems. The resulting systems may then be expected to be successfully tuned to a particular SAG mill or SAG circuit by adjusting their parameters, since the principal characteristics of these mills have been implicitly taken into account due to the involvement of the mill model in their design. Such special dynamic model is not intended for mill design nor layout designs.

The quality of automatic control performance achievable in a closed circuit grinding operation is determined to a large extent by the ability to measure circuit variables and identify disturbances. Ore grindability is often one of the most important disturbances in grinding operations but, unfortunately, the possibility of measuring grindability on-line has seemed too remote, so the possibility of taking opportune corrective actions has been thwarted.

An estimation or measurement of ore grindability is also required for an optimal operation of mining facilities. A modern approach to grinding operations in the mining industry considers mining and mineral processing operations in a holistic manner, as in the Mine to Mill methods (JKTech, 2004). Mill throughput depends on ore grindability, usually characterized off-line for some ore samples (Morrell, 2004). Another possibility is to estimate the ore grindability from lithological characterization by image analysis and on-line measurements (Casali et al., 2001). However the mill is usually fed with ores from different mine sectors and also the ore is mixed in ore pass, stock piles, and so on. To overcome this problem it is better to identify on-line the grindability of the ore in the mill, so it can be correlated with the different ore types fed to the plant and with the mill throughput. A supervisory control system may be then designed to take the SAG mill circuit to optimal operating points by acting on

* Corresponding author. Electrical Engineering Department, University of Chile, Av. Tupper 2007, Santiago, Chile. Tel.: +56 2 6784214; fax: +56 2 6720162.
E-mail addresses: gugonzal@ing.uchile.cl, gugonzal@cec.uchile.cl (G.D. Gonzalez).

the set points (e.g., of hold-up) of the lower level SAG mill circuit control systems.

Fault detection and identification (FDI) methods will be used here to detect and identify the grindability of the ore, considering that different grindabilities produce different operating conditions which, although not considered fault situations, give rise to different characteristics of measured variables, some of which may serve to estimate the grindability of the ore in the mill. The variance of the continuous wavelet transform (Daubechies, 1992; Gonzalez, 2003, 2006) of the measured plant variables has been used in FDI methods. The method developed in Gonzalez et al. (2003, 2006) has been applied here to the identification of a grindability index, but also incorporating mean values directly in order to better discriminate between operating conditions determined by the grindability indexes.

2. The SAG circuit and its model for two kinds of ore

2.1. The SAG circuit model

Following the general objective stated above a SAG mill circuit dynamic model has been adjusted using data collected from a large mineral processing plant in Chile, in order to produce results approaching those which would be obtained for actual mills. In order to test the developed method, the SAG mill circuit dynamic model has to be able to handle changes in the feed ore characteristics.

The SAG circuit consists of a SAG mill and a screen as shown in the schematic diagram of Fig. 1. The dynamic model for the SAG mill is based on the constant ore model given in Amestica et al. (1993) and Amestica et al. (1996). In this case the ore sizes to be considered have been reduced to the five intervals shown in Table 1. This is required in order to have reasonably fast runs of this dynamic model, since several runs are necessary in order to generate statistical data.

An improvement with respect to the previous model (Amestica et al., 1996) is that the model has been expanded so that it is able now to keep track of two different kinds of ore. The reason for this is that if the characteristics of the feed ore change from a type A to type B set of characteristics, the ore in the mill is initially of type A and it takes time before it is ground out to the extent that all of it exits trough the mill grate. At the same time ore type B progressively increases inside the mill until all the ore hold-up in the mill is of type B. If ore grindability may be expressed as a combination of type A and type B ores, then the model is able to handle feed ores whose grindability changes as any given function of time.

Let the feed ore flow consist of two ore types A and B having different grindabilities indexes Γ_A and Γ_B and different size distributions given by column vectors $f_A=[f_{A1}\, f_{A2}\, f_{A3}\, f_{A4}\, f_{A5}]^T$ and $f_B=[f_{B1}\, f_{B2}\, f_{B3}\, f_{B4}\, f_{B5}]^T$. The five sizes being considered are shown in Table 1. Let the proportion of ore type A in the feed be μ, and that of type B be $1-\mu$, where $0\le\mu\le 1$. Then, letting F_{sfA}, F_{sfB} (t/h) be the feed flows into the mill of ores types A and B, $F_{sfA}=\mu F_{sf}$ and $F_{sfB}=(1-\mu)F_{sf}$ (Fig. 2). Let the water feed flow to the mill be F_w (t/h).

Let $m_{A,j}, m_{B,j}$ ($j=1, 2,\ldots, 5$) be the masses of ore types A and B of size j retained in the mill, H_{sA}, H_{sB} be the hold-ups of ores of types A and B and let F_{sdA}, F_{sdB} be the corresponding mill discharge flows. Hence, the total ore mass m_j of size j is given by $m_j=m_{A,j}+m_{B,j}$ and the hold-ups of ores of types A and B and the total ore hold-up are:

$$H_{sA}=\sum_{j=1}^{n} m_{A,j},\quad H_{sB}=\sum_{j=1}^{n} m_{B,j},\quad \text{and}\quad H_s=H_{sA}+H_{sB}. \tag{1}$$

Then, if grindabilities of the incoming ore may be represented by mixing a hard ore (e.g., of type A) and a soft ore (type B), this enlarged model may deal with feed ores whose grindabilities change with time in any manner by making $\mu=\mu(t)$ be a function of time. In particular, let the type of feed ore undergo a step change from type A to type B. Then let F_{sf} be of type A — i.e., $\mu=1$ — be present for a long enough period of time such that all the ore inside the mill is of type A: $H_s=H_{sA}$. For the feed ore to change from type A to type B, μ must undergo a change from 1 to 0 so the feed ore becomes $F_{sf}=F_{sfB}$. The hold-up H_{sA} of ore type A will progressively diminish until it is completely ground out and all of it has left the mill trough its grate. At the same time the hold-up H_{sB} of ore type B will increase until a new stationary condition is attained where all the mill solids hold-up is ore type B, i.e., $H_s=H_{sB}$.

The equations governing the evolution of the masses $m_{A,j}$ and $m_{B,j}$ are obtained by the dynamic balance of masses:

$$\begin{aligned}\mathrm{d}m_{A,j} &= \mu F_{sf} f_{A,j}\mathrm{d}t + F_{srA,j}\mathrm{d}t \\ &\quad + \frac{P}{H_s}\Gamma_A\alpha_{j-1,j}m_{A,j-1}\mathrm{d}t - \frac{P}{H_s}\Gamma_A\alpha_{j,j+1}m_{A,j}\mathrm{d}t - F_{sdA,j}\mathrm{d}t\end{aligned} \tag{2}$$

$$\begin{aligned}\mathrm{d}m_{B,j} &= (1-\mu)F_{sf}f_{B,j}\mathrm{d}t + F_{srB,j}\mathrm{d}t \\ &\quad + \frac{P}{H_s}\Gamma_B\alpha_{j-1,j}m_{B,j-1}\mathrm{d}t - \frac{P}{H_s}\Gamma_B\alpha_{j,j+1}m_{B,j}\mathrm{d}t - F_{sdB,j}\mathrm{d}t.\end{aligned} \tag{3}$$

In Eqs. (2) and (3) the grinding of size i ore to size j is modelled by:

$$\frac{P}{H_s}\Gamma_A\alpha_{i,j}m_i(\mathrm{t/h}),\quad \frac{P}{H_s}\Gamma_B\alpha_{i,j}m_i(\mathrm{t/h}) \tag{4}$$

where P= mill power draft (kW) and $\alpha_{i,j}$= grinding rate from size i to size j (t/kWh) (Amestica et al., 1996), for grindability index $\Gamma=1$. Following

Table 1
Ore particle size intervals

Size	Name	Interval	Interval [mm]
1	Lumps	+4″	∞, 101.6
2	Coarse ore	−4″, +2.1″	101.6, 53.3
3	Pebbles	−2.1″, +0.5″	53.3, 12.7
4	Fine ore	−0.5″, +35#	12.7, 0.4
5	Extra fine ore	−35#	0.4, 0

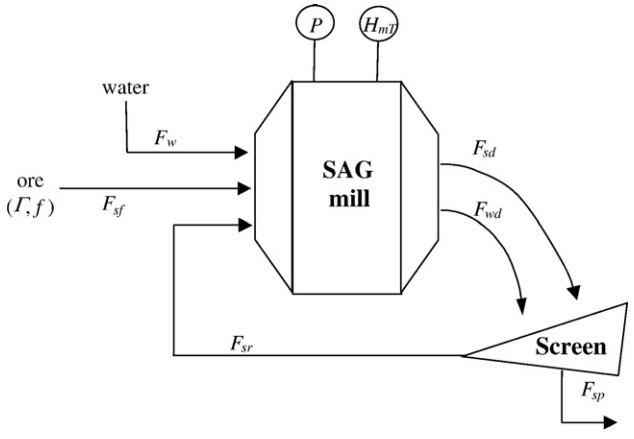

Fig. 1. Schematic diagram of the SAG circuit.

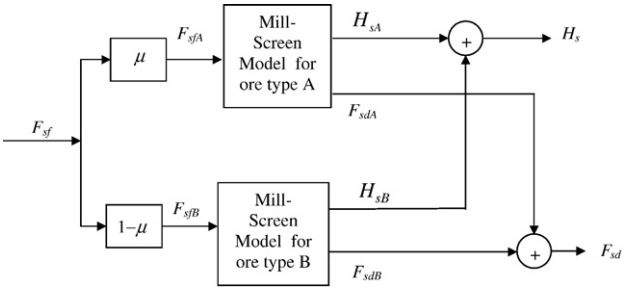

Fig. 2. Mill-screen model for handling two types of ore.

the general purpose of this model stated in the Introduction, it has been considered sufficient to account only for grinding from size i to size $i+1$.

The mill feed flows for each size j and ore type are $\mu F_{sf} f_{A,j}$ and $(1-\mu) F_{sf} f_{B,j}$, and the discharge flows for each size j are

$$F_{\mathrm{sdA},j} = \frac{(1-c_{\mathrm{g},j})Km_{\mathrm{A},j}}{\sqrt{H_{\mathrm{s}}}}, \quad F_{\mathrm{sdB},j} = \frac{(1-c_{\mathrm{g},j})Km_{\mathrm{B},j}}{\sqrt{H_{\mathrm{s}}}}, \quad j = 3, 4 \text{ and } 5 \tag{5}$$

where $c_{g,j}$ is the mill grate rejection coefficient and K adjusts the total flow presented to the grate (Amestica et al., 1993, 1996).

The return flows of ore types A and B rejected by the screen are $F_{srA,j}$ and $F_{srB,j}$ (Fig. 2) for each size j. The water hold-up H_w is given by

$$\frac{dH_{\mathrm{w}}}{dt} = F_{\mathrm{w}} - F_{\mathrm{wd}}, \quad F_{\mathrm{wd}} = \left(\lambda_0 + \frac{\lambda_1}{H_{\mathrm{s}}^4}\right) H_{\mathrm{w}} \tag{6}$$

where F_{wd} is the water discharge flow, and λ_0 and λ_1 are model fitting parameters (Amestica et al., 1993, 1996).

Shared variables in these equations for ores type A and B are the total ore feed flow F_{sf}, the power draft P and the total ore hold-up H_s.

Let the total hold-up of the mill, including water hold-up H_w, be

$$H_{\mathrm{mT}} = H_{\mathrm{s}} + H_{\mathrm{w}}. \tag{7}$$

Ore grindability is represented by a grindability index Γ in the range [0.94, 1.06], where $\Gamma = 0.94$ corresponds to hard ore, $\Gamma = 1.06$ to soft ore, and $\Gamma = 1$ to normal ore.

The particle size distribution of the feed ore is represented by four different vectors f corresponding to fine (f^{f}), normal (f^{n}), coarse (f^{c}) and very coarse (f^{vc}) size distributions.

This mill dynamic model is of the state/state-output class, resulting from the dynamic mass and water balances. The main components of the state vector are the ore masses of types A and B at the different sizes. Hence, given an initial state and the model inputs, a solution may be obtained. But, since the model in non-linear, an analytical solution is not practical, and simulation has been used.

2.2. Measured variables, disturbances and manipulated variables

The variables assumed to be measured are: F_w = water flow added to the mill input, F_{sf} = fresh solids feed flow, f = feed particle size distribution, H_{mT} = total hold-up of the mill (solids + water), F_{sr} = return ore flow — consisting mainly of pebbles — rejected by the screen, and P = mill power draft.

The disturbances considered are: v_k = white noise zero mean random disturbance affecting measurement of sensor k, w_j = white noise zero mean random disturbance added to Eqs. (2) and (3) giving ore size j in the mill, w_w = white noise zero mean random disturbance added to Eq. (6) giving the mass H_w of water in the mill, p_k = random disturbance affecting the feed particle size distribution. These random disturbances — which are stochastic processes (Papoulis and Pillai, 2002) — have been added to account for uncertainties in model and variables. In addition, the following disturbances are considered: changes in the grindability index Γ, changes in the feed ore particle size distribution, and changes in the SAG circuit characteristics (represented by changes of the circuit model parameters).

The manipulated variables of the simulator are the feed flow F_{sf} and the water flow added to the mill, F_w. Usually there is a controller that fixes the ratio of ore and water flow, in this case according to $F_{sf}/(F_{sf}+F_w)$, so the only manipulated variable in this case is the feed ore flow F_{sf}.

The screen performance is represented by rejection coefficients c_{rj} affecting the mill discharge flows of sizes $j = 3$, 4 and 5 entering the screen. Let the solids flow of size j (see Table 1) passing the screen be F_{spj} (Fig. 1). Then $F_{spj} = (1-c_{rj})F_{sdj}$, where c_{rj} is the screen rejection fraction for ore flow F_{sdi} of size i ($i = 3$, 4, 5). Sizes 1 and 2 are rejected by the mill grate, so $F_{sp1} = 0$ and $F_{sp2} = 0$. Then the rejected ore flows in Eqs. (2) and (3) for each size and ore type are $F_{srA,j} = c_{rj}F_{sdA,j}$ and $F_{srB,j} = c_{rj}F_{sdB,j}$.

The rejected ore flows F_{srA} and F_{srB} are conveyed back to the mill input where they join the new ore feed flows F_{sfA} and F_{sfB}. The mesh opening size of the screen is in this case 12.7 mm (1/2"), so that the ore size 3 is rejected by the screen ($c_{r3} = 1$), while ore size 5 passes the screen ($c_{r5} = 0$) and a fraction c_{r4} of ore size 4 is rejected. The rejection coefficient c_{r4} has been used as a model adjusting parameter. The rejected flow for ore type A is then $F_{srA} = F_{srA,3} + F_{srA,4}$, where $F_{srA,3} = F_{sdA,3}$ and $F_{srA,4} = c_{r4}F_{sdA,4}$, and similarly for ore type B. It has been assumed that water rejection by the sieve is not significant.

2.3. Adjusting the SAG circuit model to data from a real SAG circuit

The mill model was adjusted using the following nominal values for the SAG mil operation: mass of lumps $H_{s1} = 110$ (t), total mass of ore in the pulp $H_{s2} = 46$ (t), total mass of ore $H_s = 156$ (t), mass of water $H_w = 20$ (t), mass of balls $H_b = 194$ (t), equivalent porosity $\varepsilon_{eq} = 0.35$, lumps porosity $\varepsilon_l = 0.35$, balls porosity $\varepsilon_b = 0.35$, solids density $\rho_s = 2.7$ (t/m^3), ball fraction $J_b = 0.12$, slurry density $\rho_p = 1.79$ (t/m^3) and solids concentration $C_P = 0.7$ (Amestica et al., 1993, 1996). In addition, new ore feed flow $F_{sf} = 1217$ (t/h), screen rejected ore flow $F_{sr} = 134$ (t/h), and total mill ore feed flow $F_s = 1351$ (t/h). The mill diameter is $D = 9.8$ (m), its equivalent (cylindrical) length is $L = 4.6$ (m), and the mill internal volume is $V_m = 347$ (m^3). The % size distributions for the fresh feed f_f, screen rejection f_r, circuit product f_p, mill discharge f_d, and mill feed f_s streams are given by f_f = [33.0 15.0 44.0 7.9 0.1], f_r = [0.0 0.0 95.6 4.4 0.0], f_p = [0.0 0.0 0.0 49.9 50.1], f_d = [0.0 0.0 9.5 45.5 45.1], and f_s = [29.7 13.5 49.1 7.6 0.1], for the sizes in Table 1.

2.4. Response of the SAG circuit model

The SAG circuit model was used to build the SAG circuit simulator using SIMULINK from MATLAB. The simulator includes an option of PID automatic control of the total mill hold-up H_{mT}, as well as a ratio control of the feed water flow F_w in proportion to the solids feed flow F_{sf}. Using the SAG circuit simulator the response of the simulated circuit under various operating conditions has been determined.

2.4.1. Evolution of hold-ups of different ores

With the hold-up control off, and the water ratio control set at 0.63, the grindability index of the feed ore undergoes a large abrupt change from $\Gamma_A = 0.94$ (hard ore) to $\Gamma_B = 1.06$ (soft ore), at $t = 8$ (h), after the circuit had settled down following an initial transient. Fig. 3 shows how the

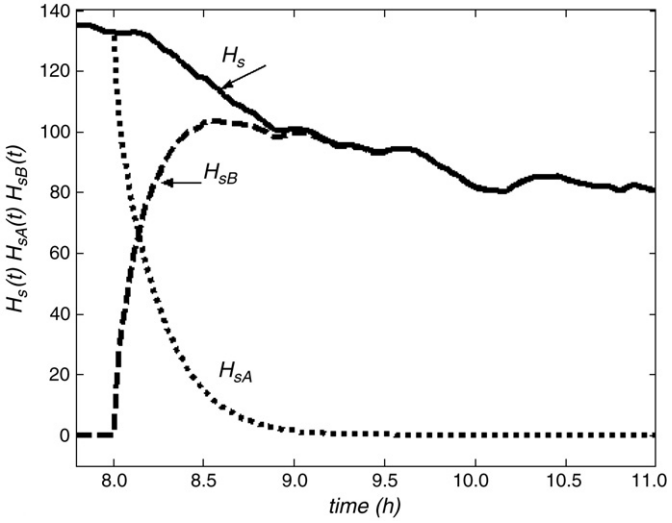

Fig. 3. As feed the grindability of the feed ore undergoes a step change at $t = 8$ (h) from hard ore (A) to soft ore (B), the hard ore progressively disappears as it is ground out, while the soft ore increases until it replaces the hard ore.

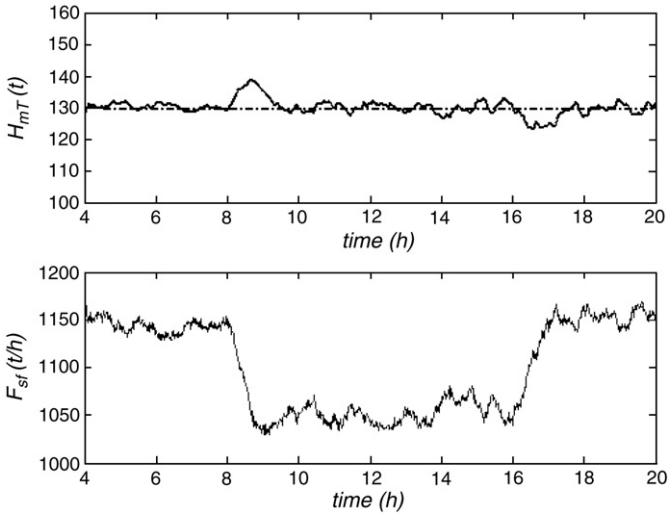

Fig. 4. The control system manipulates the feed ore F_{sf} in order to keep the hold-up H_{mT} close to its set point of 130 (t) when the feed ore changes at t=8 (h) from normal size distribution and normal grindability to hard ore with coarse size distribution and back again to normal ore at t=16 (h).

hard ore mass H_{sA} disappears as it is ground out, while the soft ore mass H_{sB} increases until it becomes the total solids hold-up H_s of the mill.

2.4.2. Automatic hold-up control

With the automatic control of hold-up H_{mT} and feed water ratio control, the feed ore changes at t=8 (h) from normal size distribution and normal grindability to hard ore with coarse size distribution. At t=16 (h) the feed ore changes back to normal again. As seen in Fig. 4 in order to maintain the hold-up close to its set point of 130 (t), the control system reduces the feed ore F_{sf} during the period where the hard ore is present in the SAG mill.

From the results obtained, e.g., Figs. 3 and 4, it may be concluded that the circuit response corresponds to that of a real circuit from a qualitative point of view, and that from a quantitative point of view is within what might be expected of such circuits. Therefore, the objective stated for this model in the Introduction may be considered to have been satisfied.

3. Detection and identification of grindability using the wavelet variance

The purpose here is to detect and identify ore grindability index Γ in the SAG circuit shown in Fig. 1 using a method based on the wavelet variance (Gonzalez et al., 2003, 2006) of measured variables defined in Section 2.2. Again, the case where automatic control of hold-up is active has been considered, together with automatic ratio control of the feed water, in order to emulate in some fashion the actions of an operator that is manually controlling the circuit, or the case where such controls are actually installed and working.

3.1. Detection and identification

Grindability detection is sensing that the grindability of the feed ore has changed. Such would be the case illustrated by Fig. 4, where the problem would be to estimate an approximate value t_d for times t_c where the changes occur, such as t_c=8(h) and t_c=16 (h), when the ore changes from medium to hard and back again to medium. A time delay $t_D=t_d-t_c$ may be tolerated, since the effect of the change in the mill operation takes place progressively as the ore changes inside the mill, as shown in Fig. 3. An important performance measure in detection is the mean detection delay $\overline{t_D}$.

Identification, on the other hand, refers here to estimating the grindability index which the ore will reach or has reached in stationary conditions, e.g., as in time interval [8, 16] in Fig. 4.

Important performance characteristics here are: (i) percentage of hits (correct identification) and of misses (miss-identification, including failure to identify), and (ii) insensitivity in the identification of a given parameter such as Γ to changes in equipment characteristics — e.g., changes of mill grate opening, ball load, screen opening, mill parameters affecting grinding — and to changes in some variables such as feed ore particle size distribution.

3.2. Detection and identification methods

Fault Identification and Detection (FDI) methods (Chen and Patton, 1999) are suitable in general for identifying operating points or detecting changes in operating points, even though no fault may be present. FDI methods may broadly be classified in (a) *Model Based FDI*, i.e., those which require a model of the plant or unit (multi-model approach (Chen and Patton, 1999)), and (b) *Feature Based FDI*, i.e., those which do not. In this latter case the different operating conditions are found by directly analyzing features of the measured variables.

The Feature Based FDI method is used here. Examples of features extracted from measured variables are, mean values, variances, auto correlation functions, cross correlation functions, etc., either of the variables themselves or of transformations performed on the variables such as Fourier transform or series, and continuous or discrete wavelet transforms.

In the present SAG circuit case the feature used is the continuous wavelet transform (CWT) variance of measured variables (Gonzalez et al., 2003, 2006). In this case this method is applied to measured variables of the SAG circuit of Fig. 1 (see Section 2.2). An overall view of such method shall be given here. Details may be found in the cited references.

The operations in this method comprise two stages: (i) feature extraction and (ii) feature processing.

3.2.1. Feature extraction

Let $y_j(\Gamma_i)$ be a measurement performed on the SAG circuit, e.g., $F_{sr}(t)$, when the ore grindability index is $\Gamma_i(t)$, and let $Z(\Gamma_i)$ be the feature extracted from a given measurement $y_j(t)$, or a combination of the features extracted from a set a set of measurements (e.g., $F_{sf}(t)$, $P(t)$, $F_{sr}(t)$), when Γ_i is known. Feature $Z(\Gamma_i)$ shall be called *characteristic template* for grindability index Γ_i for a given set of measurements, and are found off-line using experimental and historical records obtained from the plant. Feature $S_m(\Gamma)$, obtained on-line from measurement $y_j(\Gamma)$, or combining features extracted from a set of such measurements, when the grindability index Γ is unknown, shall be called *sample template*. It will be used to estimate the unknown grindability index Γ_k under the current operating conditions by comparison with the set of characteristic templates.

When the variables exhibit a stochastic nature, as in this case (e.g., see Fig. 7) feature extraction from measured variables involves expected values. This is in general difficult, and sometimes impossible, because statistical parameters and functions (e.g., joint probability densities) are required which are generally unavailable from a practical point of view. However, these expected values may be estimated by means of time averages of a single outcome of the stochastic process (Gonzalez et al., 2003, 2006).

3.2.2. Feature processing

The sample template $S(\Gamma_k)$, and the characteristic templates $Z(\Gamma_i)$ (i=1,…, m) are now processed in order to distinguish, with acceptable error, which is the prevailing condition of the plant being analysed, by finding to which characteristic template the sample template is closest to, according to a given criterion. Methods that may be used to this end are, hypothesis testing, concatenation of functions, principal

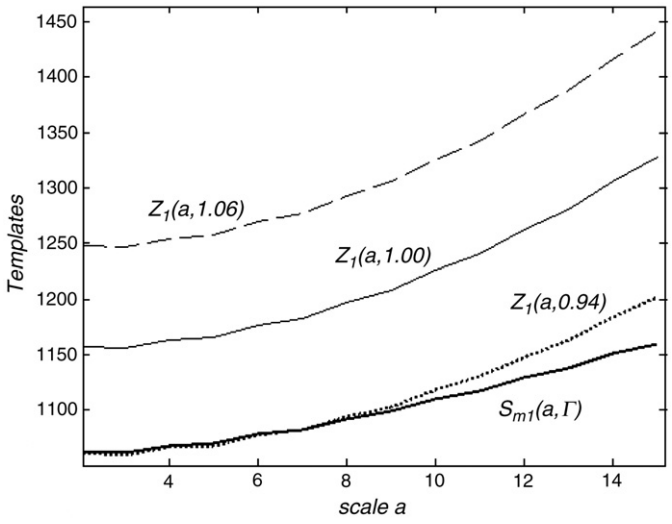

Fig. 5. Characteristic templates for feed ore flow F_{sf}: $Z_1(a, 0.94)$ for hard ore and coarse particle size, $Z_1(a, 1.00)$ for normal ore, normal particle size and $Z_1(a, 1.06)$ for soft ore and fine particle size, under normal operating conditions, and sample variance $S_{m1}(a, \Gamma)$ for F_{sf} corresponding to a given measurement when the ore in the mill is hard with coarse particle size.

component analysis (PCA), projection into the Fisher space, quadratic discriminant analysis (QDA), etc. (Mardia, 1979).

3.3. Application to SAG circuit grindability index estimation

3.3.1. Feature extraction and templates

The feature used in the method originally developed by Gonzalez et al. (2003, 2006), is the variance of the continuous wavelet transform (CWT) of measured variables (e.g., in the SAG circuit case, $F_{sf}(t)$, $P(t)$, $F_{sr}(t)$). The CWT of $y(t,\Gamma)$ is

$$W(a,b,\Gamma)=\frac{1}{\sqrt{a}}\int_{-\infty}^{\infty} y(t,\Gamma)\Psi\left(\frac{t-b}{a}\right)\mathrm{d}t. \tag{8}$$

It turns out that if $y(t,\Gamma)$ may be considered a wide sense stationary random process — at least within a time frame — then the expected value of Eq. (8) is zero and its variance only depends on scale a. Due to random nature of the variables in the SAG circuit, the proper way to consider the measured variables for a given Γ_i is as realizations — or outcomes — of a stochastic process $y(t, \Gamma_i, \xi)$ where ξ accounts for the randomness and selects one of all the possible measurements that could have been obtained because of the random nature of the variables (Papoulis and Pillai, 2002). This implies that the CWT is random and has an expected value and a variance $E\{W^2(a, b, \Gamma_i, \xi)\}=V(a, \Gamma_i)$, where $W(a, b, \Gamma_i, \xi)$ is the CWT of measured variable $y(t, \Gamma_i, \xi)$ when the grindability index is Γ_i. It turns out that (Gonzalez et al., 2003, 2006) these CWT variances V are only functions of the real variable a and of the parameter Γ and may be used as characteristic templates corresponding to operating condition determined by Γ. But $V=V(a, \Gamma_i)$ does not account for the mean of $y(t, \Gamma_i, \xi)$ (Gonzalez et al., 2006), which may be important in the identification of Γ_i. Then let the characteristic template for the jth measured variable — e.g., $F_{sf}(t)$, $P(t)$, $F_{sr}(t)$ — for operating condition Γ_i include such mean, i.e.,

$$Z_j(a,\Gamma_i)=E\left[W_j^2(a,b,\Gamma_i,\xi)\right]+E\left[y_j(\Gamma_i)\right]. \tag{9}$$

For a single measurement $y_j(t, \Gamma_k)$ made on the plant — following Gonzalez et al. (2006), let the sample template be defined as

$$S_{mj}(a,\Gamma_k)=\frac{1}{T}\int_0^T W_j^2(a,b,\Gamma_k)db+\frac{1}{T}\int_0^T y_j(t,\Gamma_k)\mathrm{d}t. \tag{10}$$

It may be shown that this sample template is an unbiased estimator of the characteristic template $Z_j(a, \Gamma)$ given by Eq. (9) (Gonzalez et al., 2006).

In the case of the SAG circuit, three basic operating conditions corresponding to three grindability indexes Γ have been chosen: (i) for hard ore with $\Gamma_1=0.94$, (ii) for medium ore with $\Gamma_2=1.00$, and (iii) for soft ore with $\Gamma_3=1.06$. Then, for each of the following measured variables indexed by j: (a) feed ore flow F_{sf}, ($j=1$), (b) power draft P, ($j=2$), and (c) rejected flow F_{sr}, ($j=3$), there are three characteristic templates $Z_j(a, \Gamma_i)$ ($i=1,2,3$).

Fig. 5 shows the three characteristic templates corresponding to feed ore flow F_{sf} (measured variable $j=1$) for hard ore ($\Gamma=0.94$) and coarse particle size, normal ore ($\Gamma=1.00$) and normal particle size, and soft ore ($\Gamma=1.06$) and fine particle size, under normal operating conditions, with automatic control of total hold-up H_{mT} active and feed water ratio control also active. Also shown is a sample variance $S_{m1}(a, \Gamma)$ for feed ore F_{sf} corresponding to a given measurement when the unknown ore is hard ($\Gamma=0.94$) with coarse particle size. It is apparent in this case that the operating condition corresponds to hard ore ($\Gamma=0.94$), since S_{m1} is closest to the hard ore characteristic template. But there are cases in which this clear-cut decision is not so easy and template processing must be resorted to, as in Gonzalez et al. (2006).

For the case of measured variable j one way to measure the closeness between a sample template $S_{mj}(a, \Gamma)$ and any characteristic template $Z_j(\Gamma_i)=Z_j(a, \Gamma_i)$ is to find the distance Δ_j between them using the square root of the integral of the squared differences, i.e.,

$$\Delta_j=\sqrt{\int_0^T\left[S_{\mathrm{mj}}(a,\Gamma)-Z_j(a,\Gamma_i)\right]^2 da}. \tag{11}$$

The problem of identifying the operating point of the plant is then to determine for which Γ_i distance Δ_j is minimum.

3.3.2. Template processing

Following the good results reported by Gonzalez et al. (2006), the three characteristic templates for Γ_i as well as the three sample templates for the unknown Γ have been concatenated, i.e., its scales axis a have been juxtaposed, as shown in Fig. 6. Let this concatenated characteristic template be $Z(a, \Gamma_i)$ and the concatenated sample template be $S_m(a, \Gamma)$ corresponding to the measured variables F_{sf}, P and F_{sr}.

Further template processing includes (i) discretisation of scales a, (ii) dimension reduction using PCA (Mardia, 1979), (iii) projection of the reduced dimension templates into the Fisher space (Mardia, 1979), and decision on the Fisher space as to which characteristic template the sample template is closest to (Gonzalez et al., 2003, 2006).

4. Results

Results have been obtained by programming both the SAG circuit model and the grindability detection and identification method using MATLAB and Simulink.

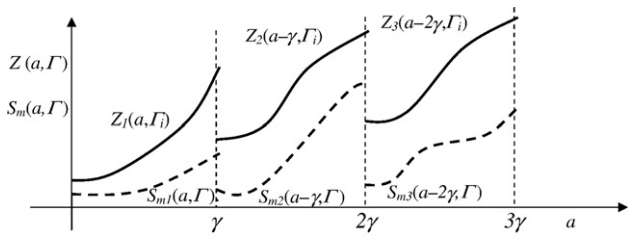

Fig. 6. Concatenated characteristic template $Z(a, \Gamma_i)$ formed by concatenating templates $Z_j(a, \Gamma_i)$, for an operating condition represented by Γ_i, for three measured variables j(F_{sf}, P, F_{sr}), when scale a is in interval $[0, \gamma]$. Also shown is a concatenated sample variance $S_m(a, \Gamma)$.

4.1. Generation of templates

For each known value of the three grindability indexes Γ_i (i.e., 0.94, 1.00, 1.06), 100 outcomes $S_{m,r}(\Gamma_i)$, $r=1$ to 100, of sample template variances were generated for each of the five values of J_b in the set {0.11, 0.12, 0.13, 0.14, and 0.15}. These $S_{m,r}(\Gamma_i)$ were determined using measurements of length $T=20$ (h) of the measured variables F_{sf}, P and F_{sr}. Then characteristic template $Z(\Gamma_i)$ has been determined by averaging these $Q=500$ sample templates for a given Γ_i (Gonzalez et al., 2006). The result is three characteristic templates which are represented by three points in the Euclidean vector space $\Re^{42}$. The projection of these templates onto the reduced PCA of dimension 8 is then projected to Fisher space of dimension 2 giving the characteristic templates $Z_F(\Gamma_1)$, $Z_F(\Gamma_2)$, and $Z_F(\Gamma_3)$ (Gonzalez et al., 2006).

4.2. Identification results

Fig. 8 shows squared distances from the sample template projected into the Fisher space for $\Gamma=0.94$ to the characteristic templates projected in that space when Γ changes from 1.00 (normal) to 0.94 (hard). The smallest distance is seen to correctly identify the unknown Γ.

4.2.1. Identification of basic grindability indexes

In this case identification was done for cases when the actual grindability index had the supposedly unknown values of 0.94, 1.00 and 1.06. One hundred repetitions of the experiment were performed — using data collected from the SAG circuit model of Section 2 — for each one of the three grindability values. The hits and misses then determine the percentages shown in Table 2, which contains identification results which include the effect of using both the mean value and template concatenation. Table 2 also has the results when only one of the three measured variables, F_{sr}, is used for determining characteristic templates and sample templates. In each of such cases the same procedure for obtaining the Fisher space as in the concatenated case is followed, but considering the CWT variances for only one measured variable, and the corresponding covariance matrix. It may be seen that when concatenation is used there is 100% correct identification of Γ, while if only one measurement such as F_{sr} is employed correct identification is at most 67.2 % (for $\Gamma=1.06$), and miss-identification attains a maximum of 34.6% when $\Gamma=1.00$ is identified as $\Gamma=1.06$. Results using only single measurements F_{sf} and P are similar to those using only F_{sr}.

The benefit of adding the mean value of the measured variables to the variances and sample variances may be seen in Table 3. It may be seen that only when using both CWT and mean value together with concatenation 100% hits is achieved. The CWT by itself only gives a maximum of 61.8% correct identification (when $\Gamma=1.06$) without concatenation, which increases to 68% with concatenation. The identification result for both CWT and mean is only 67.2% (when $\Gamma=1.06$) without concatenation, but increases to 100% when concatenation is used. Similar results are obtained for feed flow F_{sf} and power draft P.

4.2.2. Identification of grindabilities within a continuous range

Good results were achieved in the identification of grindability within a range using concatenation when the circuit was operating with ore having a grindability index Γ in the continuous range [0.94, 1.06]. In this case a linear interpolation procedure was used around the cases for $\Gamma=0.96$, 1.00, and 1.06. Pairs of actual and identified Γ, i.e. (actual Γ, Identified Γ), are (0.940, 0.940), (0.970, 0.970), (0.990, 0.997), (1.000, 1.000), (1.010, 1.003), (1.030, 1.030), and (1.060, 1.059).

Table 2
Percentages of correct and mistaken identification of Γ, for normal feed particle size distribution, using only measurement F_{sr} and concatenated characteristic templates and sample templates

Actual Γ	F_{sr} only Identified Γ			Actual Γ	Concatenated case Identified Γ		
	0.94	1.00	1.06		0.94	1.00	1.06
0.94	64.2	34.2	1.6	0.94	100	0	0
1.00	31.4	34.0	34.6	1.00	0	100	0
1.06	3.4	29.4	67.2	1.06	0	0	100

Table 3
Correct identification (hits) percentage of Γ using CWT, mean values, and both, for only F_{sr} and for the concatenated case

	Actual Γ			Actual Γ		
	0.94	1.00	1.06	0.94	1.00	1.06
Using	F_{sr} only			Concatenation		
CWT only	53.4	13.8	61.8	69.6	35.2	68.0
Mean only	64.4	32.8	67.0	60.0	20.0	60.0
CWT and Mean	62.2	34.0	67.2	100.0	100.0	100.0

4.2.3. Sensitivity in the identification of Γ with respect to deviation from nominal conditions

In an ideal case the identification method should be insensitive to changes of circuit parameters when they change from the set of nominal parameters with which the templates were determined. However, it may be expected that there will exist some sensitivity, but it should be relatively small. In order to test such sensitivity, several tests were run where a set of selected parameters whose values have been randomly chosen in each test. These parameters are c_{g4} and K in Eq. (5), and λ_o in Eq. (6) and are randomly generated from Gaussian distributions with the following means and relative standard deviations (SD/mean %): for c_{g4}, 0.25 and 15.0%; for K, 960 and 7.5%; and for λ_o, 34 and 15.0%. One hundred tests were made to obtain $S_m(\Gamma)$ when the ore in the circuit had either grindability index 0.94, 1.00 or 1.06. The results obtained for these random variations for normal particle size show the method is reasonably insensitive. In fact, correct identification percentages of grindability index Γ for normal particle size using concatenation, were been found to be between 99.0% and 98.8%, while mistaken identification varied from 0.0% to 1.2%. The results for intermediate and coarse feed size are similar.

4.3. Detection results

Fig. 7 shows the evolution of the measured variables when feed ore changes, at $t=10$ (h), from normal ($\Gamma=1.0$) to hard ($\Gamma=0.94$). The feed ore flow F_{sf} is seen to decrease due to the action of the hold-up control

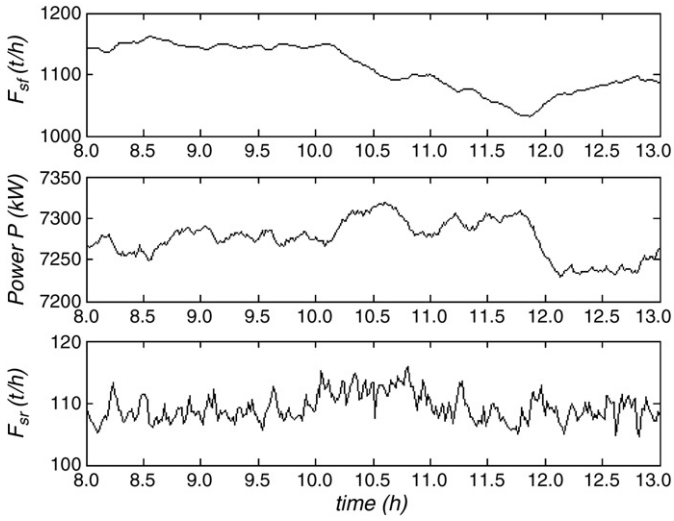

Fig. 7. Measured variables when a step change in the grindability index Γ from 1.00 to 0.94 happens at $t=10$ (h).

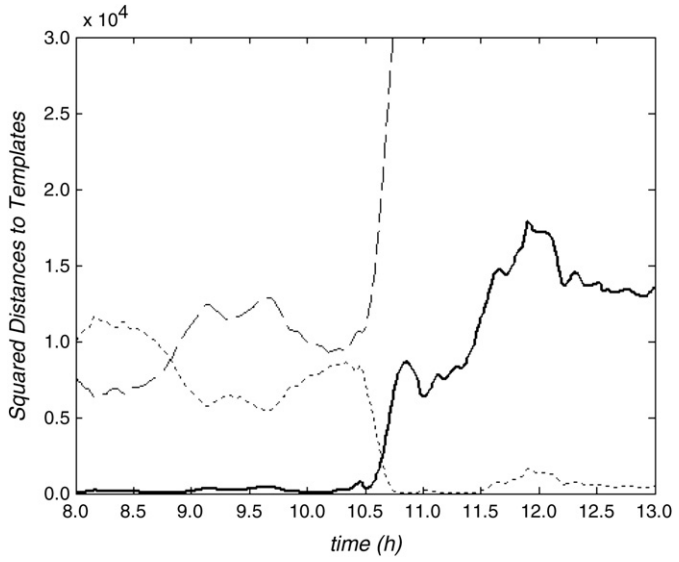

Fig. 8. Squared distances in the Fisher space between the projected sample template to the three projected characteristic templates when Γ undergoes a step change from normal (Γ=1.00) to hard (Γ=0.94) at t=10 (h). The dotted line is the squared distance from the sample template to the characteristic template for grindability Γ=0.94. The solid line and the segmented line are the squared distances from the sample template to characteristic templates for Γ=1.00 and Γ=1.06.

system in order to keep the total hold-up close to its fixed set point. Fig. 8 shows in the Fisher space the corresponding squared distances from the sample template and the three characteristic templates for hard, medium and soft ore. Mean detection delay $\overline{t_D}$ is determined here (see Section 3.1) by averaging several test results for detection times t_D. The detection delay may be handled by means of a forgetting factor λ (Ljüng, 1987; Gonzalez et al., 2006) which ponders past data in an exponentially degreasing form. The greater λ, the greater the mean time between false detections — which is a good feature — but also the greater the detection time — which is undesirable. A compromise between rapid detection and low probability of false detection was reached by using a forgetting factor λ=0.96. Mean detection times $\overline{t_D}$ for all possible step changes Γ between the three basic grindability indexes are: from 1.00 to 1.06, 62 (min); from 1.06 to 1.00, 33 (min); from 1.00 to 0.94, 36 (min); from 0.94 to 1.00, 58 (min); from 0.94 to 1.06, 78 (min); and from 1.06 to 0.94, 42 (min).

5. Conclusions

The behaviour of the dynamic model of reduced dimension developed here has shown to be good from a qualitative point of view, since its response is similar to that of actual SAG mill circuit.

Concatenation of the characteristic templates, as well as of the sample templates, has resulted in important improvements in the identification of the grindability index, as compared with the cases in which templates for only a single measurement are used.

The detection and identification method considering the mean value of the measured variables, in addition to the variance of their continuous wavelet transform, has produced a considerable improvement in the identification of the ore grindability in all cases. For example, even with the help of concatenation, the correct identification percentages of normal ore type are 35% when only CWT variances are used, and 20% if only mean values of the measured variables are used. However, if both are taken into account this percentage increases to 100%.

The method was found to be reasonably insensitive to variations of some selected parameters, as expected due to the design.

Detection of a step change of grindability of the incoming ore has been found to take from somewhat more than 30 min to a maximum of 78 min for an extreme ore change.

The estimation of the grindability index may serve for a supervisory control (or an experienced operator) acting mainly on the fresh ore feed set point, to drive the circuit to desired operating points. Such action may be improved using measurement or estimation of other variables, e.g., feed size, ball loading.

It should be clear that the method developed here may be used not only for detecting and identifying other operating conditions in a SAG circuit, but for fault detection and identification in other plants of the minerals industry as well as in other industries.

Acknowledgements

Research leading to this paper has received funding from Project FONDECYT 1020741, and from the Departments of Mining and of Electrical Engineering of the University of Chile.

References

Amestica, R., Gonzalez, G., Menacho, J., Barria, J., 1996. A mechanistic state equation model for a semiautogenous grinding mill. International Journal of Mineral Processing 44–45, 349–360.

Amestica, R., Gonzalez, G., Barria, J., Magne, L., Menacho, J., Castro, O., 1993. A SAG mill circuit dynamic simulator based on a simplified mechanistic model. In: Woodcock, J.D. (Ed.), AIMM, Proceedings XVIII International Mineral Processing Congress, Sydney, Australia, vol. 1, pp. 117–130.

Casali, A., Gonzalez, G., Vallebuona, G., Perez, C., Vargas, R., 2001. Grindability soft-sensors based on lithological composition and on-line measurements. Minerals Engineering 14 (7), 689–700.

Chen, J., Patton, R.J., 1999. Robust Model-based Fault Diagnosis for Dynamic Systems, first ed., Kluwer Academic Publishers.

Daubechies, I., 1992. Ten lectures on wavelets. CBMS-NSF Regional Conf. Series in Applied Mathematics, vol. 61. SIAM, p. 24.

Gonzalez, G.D., Paut, R., Cipriano, A., Miranda, D., Ceballos, G., 2006. Fault detection and isolation using concatenated wavelet transform variances and discriminant analysis. IEEE Trans. Signal Processing vol. 54 (5), 1727–1736 May.

Gonzalez, G.D., Ceballos, G., Paut, R., Miranda, D., La Rosa, P., 2003. Fault detection and identification through variance of wavelet transform of system outputs. In: Mastorakis, N.E., Manikoupoulos, C., Antoniou, G.E., Mladenov, V.M., Gonos, I.F. (Eds.), Recent Advances in Intelligent Systems and Signal Processing. WSEAS Press, pp. 47–53.

JKTech, 2004. Mine-to-Mill. www.minetomill.com.

Ljüng, L., 1987. System Identification; Theory for the User, first ed. P. T. R. Prentice Hall, New Jersey, USA.

Mardia, K.V., Kent, J.T., Bibby, J.M., 1979. Multivariate Analysis, first ed. Academic Press.

Morrell, S., 2004. Predicting the specific energy of autogenous and semi-autogenous mills from small diameter drill core samples. Minerals Engineering 17 (3), 447–451.

Papoulis, A., Pillai, S.U., 2002. Probability, Random Variables, and Stochastic Processes, fourth ed. McGraw-Hill.